Investigation of Two-Dimensional Shock-Wave/Boundary-Layer Interactions

Stanley A. Skebe*
United Technologies Research Center, East Hartford, Connecticut
Isaac Greber†
Case Western Reserve University, Cleveland, Ohio
and
Warren R. Hingst‡
NASA Lewis Research Center, Cleveland, Ohio

This paper reports results of experiments on the interaction of oblique shock waves with flat-plate boundary layers in the 30.48 × 30.48 cm (1 × 1 ft) supersonic wind tunnel at the NASA Lewis Research Center. These experiments were directed toward providing well-documented information of high accuracy useful as test cases for analytical and numerical calculations. Measurements of the plate surface static pressure and shear stress distributions as well as boundary-layer velocity profiles were obtained through the interaction region. Other measurements were also performed in order to document the tunnel test section flowfield and the two-dimensionality of the interaction regions. The findings presented provide detailed description of two-dimensional interactions with initially laminar boundary layers over the Mach number range 2.0–4.0. Additional information with regard to interactions involving initially transitional boundary layers was obtained at Mach numbers of 2.0 and 3.0 and those for initially turbulent boundary layers at Mach 2.0. Flow conditions encompassed a Reynolds number range of 4.72×10^6–2.95×10^7/m. These findings represent the most complete and detailed set of experimental information on oblique shock-wave/laminar boundary-layer interactions over the Mach number range 2.0–4.0. The data are available in digitized format for test case applications. Where comparison was possible, the shock/boundary-layer interaction results were found to be generally in good agreement with the experimental work of previous authors, both in terms of direct numerical comparison and in support of correlations establishing laminar separation characteristics.

Nomenclature

A, B, C, D, E, F = label to indicate axial location of velocity profile
C' = τ_w/Q_∞
$\tilde{C}_f$ = ratio of $(\tau_w/Q_\infty)_0$ at given R_{x_0} to corresponding value at $R_{x_0} = 10^6$
C_{FG} = $(\tau_w/Q_\infty) \cdot \left[\sqrt{R_x}/\sqrt{R_{x_g}}\right]$
ℓ = length of separation pressure plateau
ℓ' = separation length based on distance between shear stress fit "zero" values
L = axial location of shock impingement
L_{ref} = nominal tunnel dimension, defined to be 30.48 cm (12.000 in.)
M = Mach number
N = geographic direction: north
P = pressure
P' = P/P_{st}
$\overline{P}$ = $(P - P_0)/(P_0 \cdot \sqrt{\tilde{C}_f})$
Q = dynamic pressure
R = Reynolds number based on freestream conditions
R/ℓ = unit Reynolds number based on freestream conditions
U = axial component of mean flow velocity
U' = U/U_e
W = geographic direction: west
x, y, z, X, Y, Z = coordinate dimensions
X' = $(x - x_s)/XD$
XD = length of interaction region
Y' = $[y \cdot \sqrt{R_x}]/x$
θ = shock generator angle with respect to plate
σ = standard deviation
τ = shear stress

Subscripts

e = conditions in local freestream at axial location
F = conditions at location at end of interaction
G = conditions of Ref. 15
pl = plateau
rise = ratio of pressures at end and start of interaction
s = separation point
st = stagnation conditions in plenum
w = wall
x = axial distance downstream from plate leading edge
y = distance normal to plate surface
∞ = freestream conditions upstream of model
0 = conditions at start of interaction pressure rise

Received Sept. 7, 1984; revision received June 30, 1986.

*Associate Research Engineer, Experimental Gas Dynamics Section. Member AIAA.
†Professor, Department of Mechanical and Aerospace Engineering. Associate Fellow AIAA.
‡Aerospace Engineer, Aerodynamics Branch.

Introduction

ADVANCEMENTS in computational capability over the past decade have made analytical and numerical procedures increasingly more sophisticated to the point that solutions of complex flow problems, such as three-dimensional supersonic flows with wave interactions and separated regions, will soon be possible. Along with these advancements, however, is the need for more complete and accurate sets of experimental data, obtained from fundamental configurations, against which the calculational procedures can be tested.

Numerous experiments have been performed on flows involving interactions between boundary layers and shock waves since their observation more than 40 years ago.[1] Early pioneering studies[2-5] together encompassed a variety of flow configurations and test conditions, investigating both normal and oblique shock impingements on surfaces possessing laminar, transitional, and turbulent boundary layers. These early works emphasized the deduction of a qualitative understanding of the interaction process over a range of conditions. More recent studies[6-9] have been more specialized, with quantitative examination of specific interaction conditions as their objective.

With regard to laminar flat-plate boundary layers interacting with oblique shocks, a set of fairly detailed results[6] has been applied extensively by numerous authors[10-12] as test cases for numerical schemes and for correlations. Although these experiments were carefully performed, they lack the degree of documentation of measurement accuracies and tunnel flow characteristics that are appropriate for testing numerical solutions. Also, these experiments examined only Mach number 2.0.

The goal of the current investigation was to fill the need for a suitable high-quality and well-documented data base on oblique shock/laminar boundary-layer interactions (see Fig. 1). Sets of data similar to those of Ref. 6 were sought, but over a range of Mach numbers and with close attention to accuracy and documentation. Steps taken to achieve definitive information included repetition of tests, redundancy of measurements, and careful examination of errors throughout the data acquisition and reduction process. Characteristics of the host wind tunnel were documented, including the extent of two-dimensionality in the region where the interaction experiments were performed. Flow properties measured within the interaction included the plate boundary-layer velocity profiles and the static pressure and shear stress distributions. Data were obtained for a wide variety of interaction strengths and flow conditions over the Mach number range 2.0–4.0. Limited results were also obtained for interactions involving initially transitional and turbulent boundary layers.[13]

Experimental Method

The experiments were carried out in the 30.48×30.48 cm supersonic wind tunnel at the NASA Lewis Research Center at Mach numbers of 2.0–4.0 and freestream unit Reynolds numbers of 3.46×10^6 to 3.07×10^7 per meter. A sketch of the facility is shown in Fig. 2. It is an open-circuit tunnel, providing continuous operation by maintaining an upstream supply of high-pressure air and a downstream subatmospheric exhaust. For each Mach number, an individual fixed-nozzle assembly, which includes the test section, is used. Reynolds number control is obtained by adjustment of the stagnation pressure in the upstream plenum chamber. Temperature of the dried and filtered supply air, although not adjustable, is typically near the ambient atmospheric value. However, neither condensation nor liquefaction occurred for any of the conditions encountered. A schlieren system for flow visualization and a traversable sting mount for positioning the measurement probes are available in the test section area. A complete description of the facility and its associated hardware is provided in Ref. 13.

Flow properties measured were total temperature and static and total pressure. Total temperatures were determined by thermocouple voltages, using an oven reference point and National Bureau of Standards (NBS) data tables for their conversion. Pressure values were obtained by means of microprocessor controlled multiple-input sequencing valves (Scanivalves) and dedicated transducers. Sequencing valve accuracy was enhanced by using limited-range differential transducers referenced to a floating representative test section pressure. All pressure transducers were calibrated against standards having NBS traceable accuracy. Some flow velocities were deduced by use of single-element hot-wire probes, of free-wire and embedded-wire designs, operated as constant-temperature anemometers.

All measurement instrumentation were linked to a minicomputer for data acquisition, conversion, display, and recording. The minicomputer was also used to control the movement of the probes.

The program encompassed three principal areas of research: a documentative study of the empty tunnel, quanti-

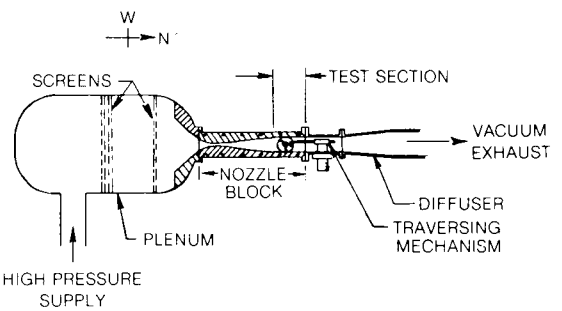

Fig. 2 NASA Lewis 1 × 1 ft supersonic tunnel cross-sectional view.

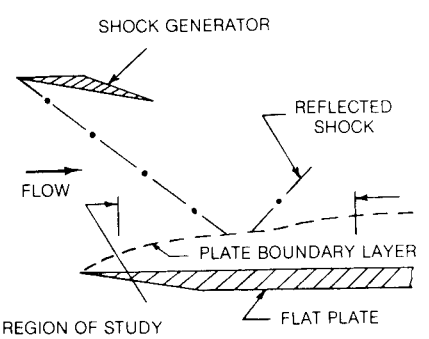

Fig. 1 Shock/boundary-layer experiment configuration.

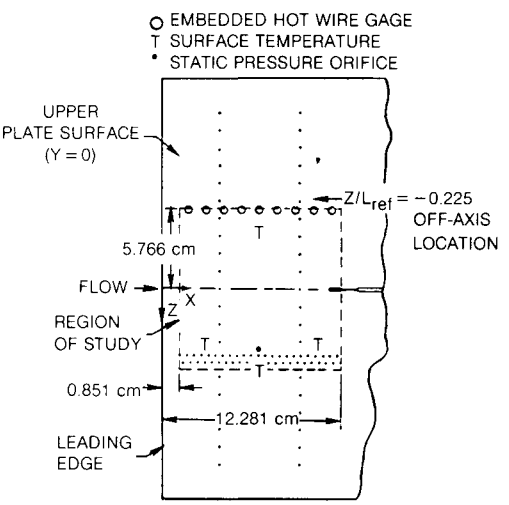

Fig. 3 Flat-plate instrumentation layout.

tative and qualitative information to validate the two-dimensionality of the geometry and flow conditions, and the quantitative investigation of shock/boundary-layer interactions.

Documentation of Empty Tunnel Conditions

A detailed investigation was performed to determine the distributions of static pressure, total pressure, and Mach number throughout the test section with no model present. Additional information obtained included a measure of freestream turbulence intensity.

Static and total pressures were measured using separate 11 element rakes, mounted on a downstream sting mount. Under computer control, each rake surveyed a set of 63 x-y and 11 z positions for a total of 693 point locations. Mach number distributions were calculated from the local static and total pressures measured at each grid point. A measure of freestream turbulence intensity in the test section was obtained using a single-element hot-wire probe, with its wire positioned to sense axial mass-velocity fluctuations.

Documentation of Two-Dimensionality

A number of qualitative and quantitative tests were made to verify two-dimensionality of the shock/boundary-layer interaction within the region of study (see Fig. 3). These tests included obtaining model and tunnel surface flow visualization patterns, plate spanwise static pressure distributions, and Stanton shear stress and boundary-layer profile data measured at on- and off-axis spanwise locations.

Flow visualization was by means of a fluorescing oil film. This technique was used to study surface patterns over the full range of Mach number, Reynolds number, shock strength, and probe position.

Plate spanwise pressure distributions were obtained by measurement of 20 taps uniformly spaced along a line parallel to the plate leading edge, at each of two axial locations within the instrumented region. These distributions gave quantitative indication of the uniformity and extent of the two-dimensional zone and the effect of interaction strength on modification of this zone. A full description of the experimental apparatus and procedures appears in Ref. 13.

Shock/Boundary-Layer Experiment

Complete sets of detailed quantitative information in the vicinity of interactions of two-dimensional oblique shocks with flat-plate boundary layers were obtained for a variety of shock strengths and flow conditions. The parameters measured included the plate surface static pressure and total temperature, total pressure of the flow throughout the boundary layer, and indirect measures of the U velocity within the linear region of the boundary-layer profile near the plate surface from both hot-wire voltage and Stanton probe pressure values.

The basic geometry of the experimental model is shown in Fig. 1. The model consisted of a bracket-mounted full-span flat plate and a full-span shock generator of triangular cross section. The flat plate and shock generator, both with ground surfaces and sharp leading edges, were fixed vertically to satisfy the functional constraints of the test section. Three separate shock generator locations were used to keep the oblique shock wave impingement near the center of the instrumented portion of the plate surface over the full Mach number range.

The shock generator was of sufficient chord length (10.16 cm) to develop a uniform compression region on the instrumented plate surface over an axial distance of 5.08–10.16 cm. This provided a margin against the upstream influence from the generator's trailing edge expansion wave of 10–60 boundary-layer thicknesses for a typical separated interaction. The shock generator was controlled by a pair of remotely activated drive units and its angle with respect to the plate surface (shock strength) determined by calibrated potentiometer output.

Measurement devices were arranged on the forward region of the plate surface, as shown in Fig. 3, where the boundary layer was expected to be laminar and two-dimensional.

The plate axial static pressure was obtained from 46 taps positioned in close proximity to one another along a line parallel to, but offset from, the plate axial centerline within the generated two-dimensional interaction region. This offset permitted simultaneous measurement of plate static and probe total pressure data throughout the region, without interference of the probe on the static pressure distribution, enabling frequent sampling of the plate static pressures. The measured static pressures were corrected for plate waviness using two-dimensional small-perturbation theory; these corrections were significant only for data near the plate leading edge. The static pressure distribution was then obtained by fitting a smoothed cubic spline to within the 1σ uncertainty in these values.

The axial shear stress on the plate surface was indirectly determined from total pressure measurements made by the probe while in contact with the plate surface at about 20 axial locations in the interaction region; the distribution was obtained by fitting a smoothed cubic spline to within the 1σ uncertainty in the data. The probe was calibrated for use as a Stanton probe based on theoretical flat-plate results for the zero pressure gradient conditions. Conditions encountered in the current study extend the region to which this technique has been applied in laminar boundary layers beyond the Mach 2.0 limit previously investigated,[14] with results suggesting a 3/4 power law for probe calibration between Mach 2.5 and 4.0. The calibration results were in agreement at Mach 2.0. with the 3/5 laminar power law and 3/4 turbulent power law established previously by Ref. 14. Additional axial shear stress data was obtained from the nine embedded hot-wire gages mounted flush with the plate surface and positioned along a line parallel to and offset from the plane axial centerline, again to allow interference-free simultaneous measurements to be made. Calibration of these gages was likewise by means of theoretical flat-plate results for the zero pressure gradient condition. Comparison of measured and theoretical zero pressure gradient profiles indicated that their modified form factors match to within 5%, with good agreement in their shapes at the wall. Hence, the Stanton probe computed shear stress values are believed to be correct to within their quoted accuracies despite the indirect method of calibration used.

Plate surface temperature was measured by four flush-mounted thermocouples. As these all gave nearly equal readings at each flow condition, the value used was the mean of the four readings. Plate temperature was generally 6% lower than the calculated adiabatic wall temperature.

Boundary-layer profiles were obtained with a flat-tipped total pressure probe mounted to and actuated by a downstream sting. Movement through the plate boundary layer from freestream to wall contact was by a computer-controlled set of discrete steps. Probe location off the plate surface was indirectly established by calibrated potentiometer output. Velocity profiles were calculated using the Crocco relation for an isothermal flat plate and for a perfect gas with specific heat ratio of 1.4 and Prandtl number of unity. Required pressures were obtained from the axial static pressure distribution.

Complete sets of data were taken at the lowest and highest Reynolds number conditions attainable for each of the 2.0, 3.0, and 4.0 freestream Mach numbers. A "complete set" consisted of velocity profiles and wall shear stress and static pressure measurements taken at a number of axial locations within an interaction established by a fixed shock generator angle and flow condition. Multiple sets were obtained at each flow condition by adjustment of generator angles to produce zero pressure gradient, weak interaction, incipient separation, and small and large separated region conditions.

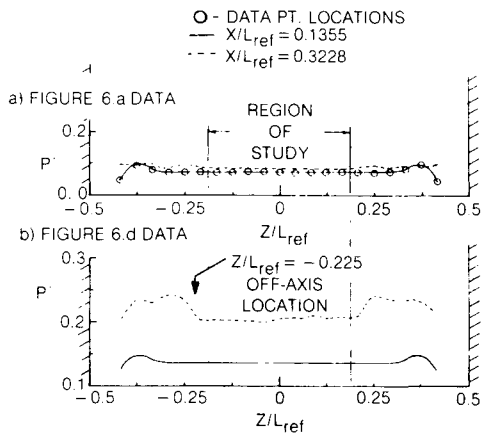

Fig. 4 Spanwise surface pressure distribution.

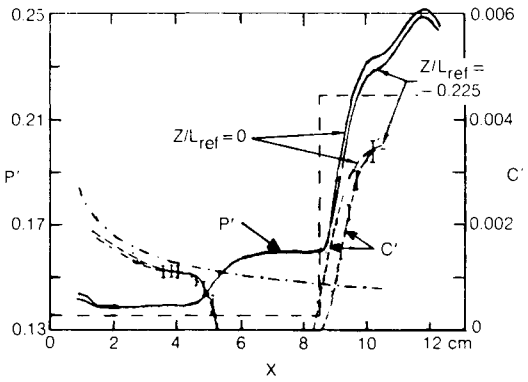

Fig. 5 Comparison of distributions at $Z/L_{ref} = 0.0$ and -0.225 for data of Fig. 6d.

Results and Discussion

Tunnel Survey

Results of the independent static and total pressure surveys of the test section volume indicated a relatively constant distribution throughout for all Mach number nozzles. Uniformity was typically within $\pm 1.5\%$ at axial stations in the volume and $\pm 3.0\%$ overall.

The uniformity of the Mach number throughout the test section volume surpassed that found for the pressures, with variation within axial stations less than $\pm 0.5\%$ and an overall uniformity of $\pm 1.4\%$.

Based on the freestream hot-wire measurements obtained, turbulence intensity is estimated to have a mean value of 0.002 and a maximum of 0.005 for all conditions encountered. Oil film patterns and the uniformities in pressure and Mach number quoted suggest flow angularity to be within ± 1 deg of tunnel centerline.

Documentation of Two-Dimensionality

The most comprehensive investigation of the extent of two-dimensionality in the shock/boundary-layer interaction experiments was performed at Mach 2.0, since wave angles and Reynolds numbers were the largest encountered and hence the resulting two-dimensional regions the smallest.

Flow visualization surface oil film patterns obtained over the range of operating conditions for which data are presented showed straight impingement or separation and reattachment lines across almost the entire plate span, indicating two-dimensional interactions. Axial oil streaks on the plate surface remained axial downstream of impingement lines within the region of study.

Quantitative data supporting two-dimensionality is presented in Figs. 4 and 5. In Fig. 4, spanwise static pressure data

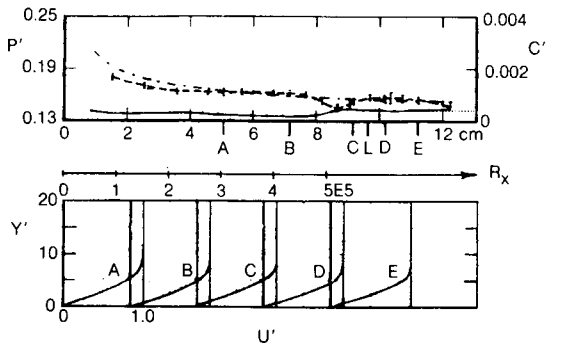

a) $M_\infty = 1.967$, $P_{st} = 48.19$ kPa, $R/\ell = 6.00 \times 10^6$/m, $\theta = 0.00$ deg, $P_{rise} = 1.045$.

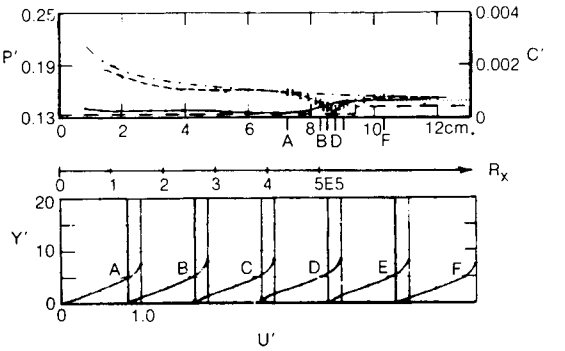

b) $M_\infty = 1.968$, $P_{st} = 48.22$ kPa, $R/\ell = 6.04 \times 10^6$/m, $\theta = 0.56$ deg, $P_{rise} = 1.100$.

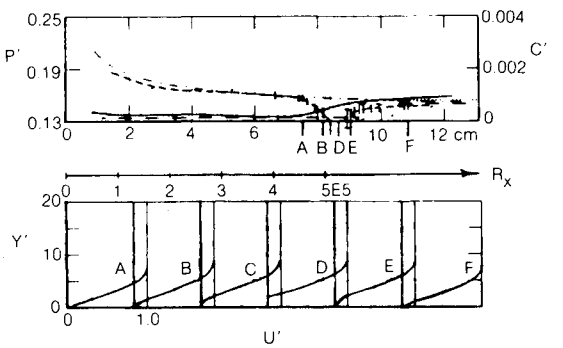

c) $M_\infty = 1.966$, $P_{st} = 48.22$ kPa, $R/\ell = 6.08 \times 10^6$/m, $\theta = 1.00$ deg, $P_{rise} = 1.137$.

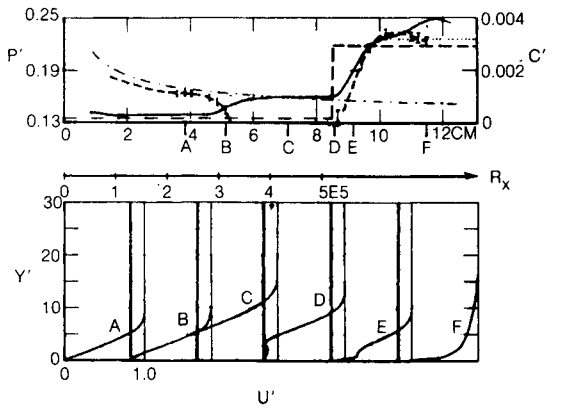

d) $M\infty = 1.963$, $P_{st} = 48.23$ kPa, $R/\ell = 6.13 \times 10^6$/m, $\theta = 4.52$ deg, $P_{rise} = 1.617$.

Fig. 6 Shock/boundary-layer interaction at Mach 2.0.

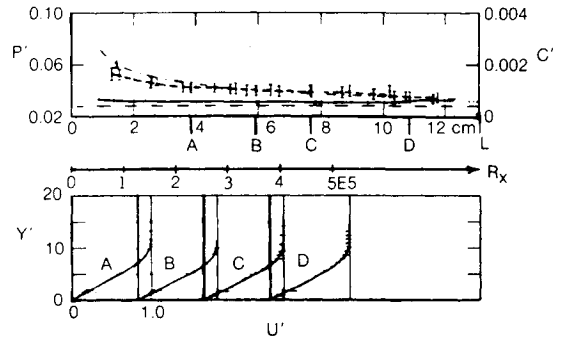

a) $M_\infty = 2.978$, $P_{st} = 79.25$ kPa, $R/\ell = 5.98 \times 10^6$/m, $\theta = 0.00$ deg, $P_{rise} = 1.048$.

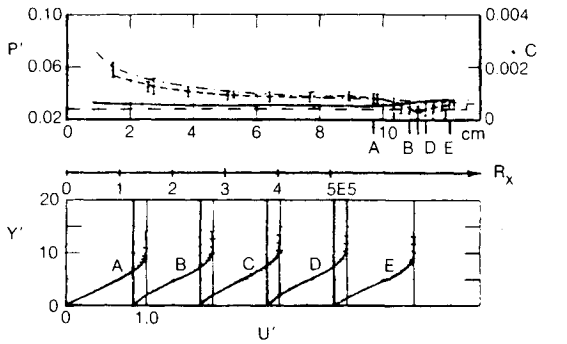

b) $M_\infty = 2.980$, $P_{st} = 79.23$ kPa, $R/\ell = 5.99 \times 10^6$/m, $\theta = 1.00$ deg, $P_{rise} = 1.153$.

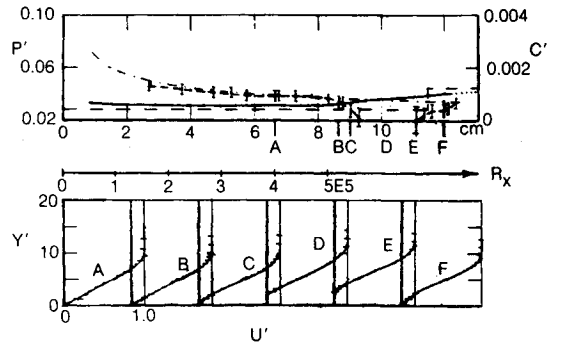

c) $M_\infty = 2.975$, $P_{st} = 79.29$ kPa, $R/\ell = 6.02 \times 10^6$/m, $\theta = 3.10$ deg, $P_{rise} = 1.372$.

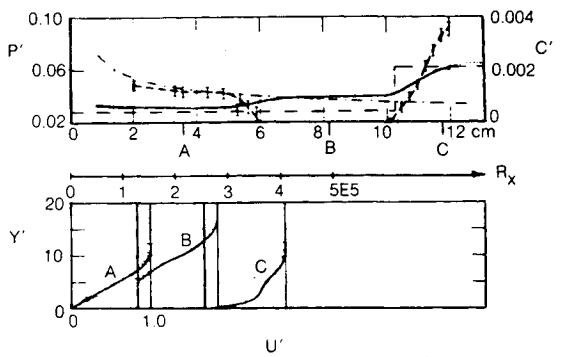

d) $M_\infty = 2.976$, $P_{st} = 79.31$ kPa, $R/\ell = 6.04 \times 10^6$/m, $\theta = 5.48$ deg, $P_{rise} = 2.078$.

Fig. 7 Shock/boundary-layer interaction at Mach 3.0.

obtained at both axial locations is displayed for both a weak and a strong $M = 2.0$ interaction. The static pressure is seen to be nearly constant across the plate within the region of study, even downstream of the separated interaction, as shown by the dashed curve in Fig. 4b. The zones of high static pressure at the ends of the spanwise distributions and their lateral growth with increase in axial distances was due to propagation of tunnel wall boundary-layer/plate leading-edge interaction disturbances. Except for interference on several downstream axial static pressure taps at Mach 2.0, the flow was unaffected by these disturbances and remained two-dimensional within the region of study.

Figure 5 compares on- and off-axis shear stress distributions. Their good agreement gives further quantitative support that the flow is two-dimensional. Correspondingly, on- and off-axis velocity profiles also showed close agreement. Therefore, high confidence of two-dimensionality was established for the interaction data. Repeatability of all quantitative measurements was also observed to be excellent.

Shock/Boundary-Layer Experiment

Figures 6–8 present graphs of quantitative results obtained for shock wave interactions with laminar boundary layers at Mach number 2.0, 3.0, and 4.0. For each interaction condition, the associated plate surface static pressure (solid line) and shear stress distribution (dashed line) are displayed on an upper grid as a function of distance from the leading edge and of Reynolds number based on this distance, while corresponding velocity profiles obtained at the indicated axial locations are presented on the paired lower grid. Velocity and shear stress data points for which negative values were obtained are excluded, as their absolute magnitudes could not be resolved directly with the instrumentation used.

Shown in each of the distribution plots for comparison are the theoretical flat-plate zero pressure gradient laminar shear stress distribution (represented by a dash-dot line) and the theoretical plate axial static pressure rise associated with the inviscid incident and reflected shock pattern (long dash line). This shock pattern was calculated from the calibrated geometric orientation of the shock generator leading edge and plate surface using inviscid two-dimensional wave mechanics.

Deviation of the actual static pressure rise from that of the theoretical was due to several factors. High static pressures were observed near the leading edge due to the induced pressure caused by boundary-layer growth. The plate static pressure then approached the freestream theoretical value, but remained slightly higher due to presence of the model, causing a slight convergence of the tunnel flow. This effect was more noticeable for the Mach 3.0 geometry than that encountered at Mach 2.0 or 4.0. Also, downstream of the interaction, the actual static pressure reached a final value higher than the computed rise. This difference was due to the effective increased incident and reflected wave angles resulting from boundary-layer displacement on the shock generator and flat plate, respectively. In addition, as the theoretical rise was based on a shock generator angle deduced from an "unloaded" calibration, the actual angle resulting from aerodynamic loading was different in some cases. For this reason, it is recommended that the actual pressure rise be used as the correlating parameter rather than shock generator angle.

Figure 6 presents results for a Reynolds number of 6.1×10^6/m at Mach 2.0, with the near-zero pressure gradient case shown in Fig. 6a. One sees that upstream of the very weak interaction the surface pressure is nearly constant, and that the skin-friction coefficient approaches the theoretical zero pressure gradient value. The velocity profiles are seen to be self-similar. Two characteristics unique to the Mach 2.0 model geometry are seen in this static pressure distribution. A slight pressure rise near $X = 4$ cm results from flow convergence due to shock generator/plate proximity, but the effect is local to only this axial position and the plate static pressure is observed to return to its undisturbed value well ahead of the

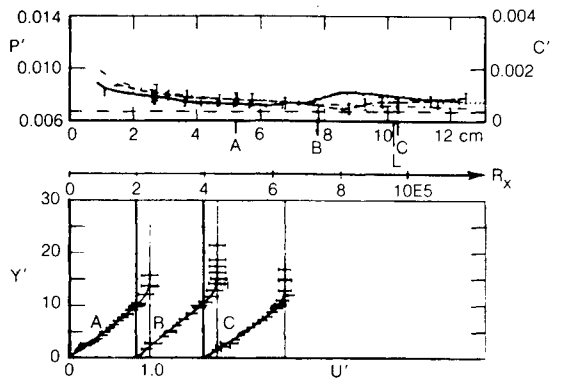

a) $M_\infty = 3.985$, $P_{st} = 206.84$ kPa, $R/\ell = 9.39 \times 10^6$/m, $\theta = 0.00$ deg, $P_{rise} = 1.032$.

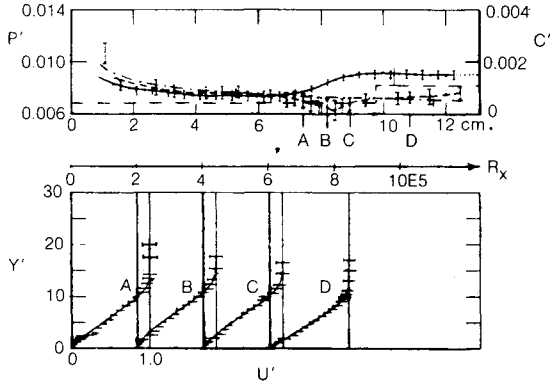

b) $M_\infty = 3.972$, $P_{st} = 206.83$ kPa, $R/\ell = 9.51 \times 10^6$/m, $\theta = 0.90$ deg, $P_{rise} = 1.227$.

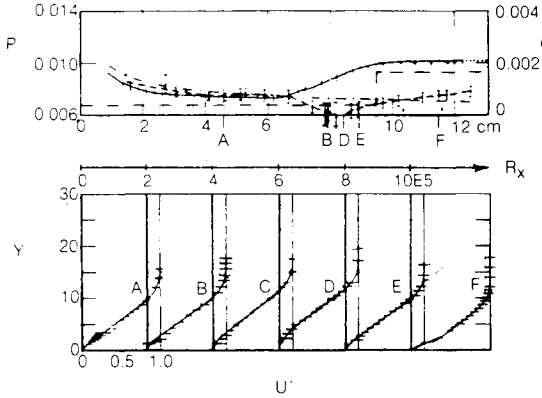

c) $M_\infty = 3.980$, $P_{st} = 206.84$ kPa, $R/\ell = 9.47 \times 10^6$/m, $\theta = 1.63$ deg, $P_{rise} = 1.397$.

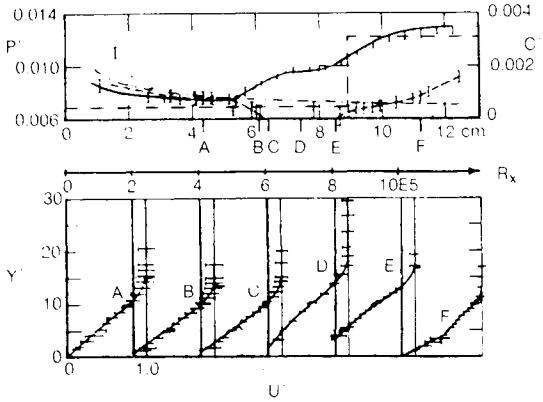

d) $M_\infty = 3.967$, $P_{st} = 2.06.82$ kPa, $R/\ell = 9.54 \times 10^6$/m, $\theta = 3.00$ deg, $P_{rise} = 1.748$.

Fig. 8 Shock/boundary-layer interaction at Mach 4.0.

interaction region. The second anomaly is that the static pressure curve does not remain at a constant final value downstream of the interaction, but instead continues a slow rise. This behavior is a result of the tunnel wall boundary-layer/plate leading-edge interaction disturbance, as discussed earlier, propagating along a Mach line near the downstream pressure taps and imposing an induced pressure on them. The true final pressure rise, which would be recorded if this disturbance were not present, is indicated by a dotted line.

Corresponding data for an interaction producing a near-incipient separation are shown in Fig. 6b. The boundary layer is essentially undisturbed except for a small neighborhood near the shock impingement point, as evidenced both by the skin-friction distribution and velocity profiles.

An interaction with a stronger shock wave, causing a small separated region, is shown in Fig. 6c. Despite the separation and reattachment, the disturbance to the boundary layer is relatively minor. The boundary layer both upstream and downstream of the interaction region retains its zero pressure gradient self-similarity. Separation is confirmed by profile D.

The most severe interaction obtained at this freestream Reynolds number is found in Fig. 6d. Here, the shock is found to cause an extended separated region upstream of its impingement location and a well-defined separation plateau pressure is observed. Also, resulting from this strong interaction, the boundary layer undergoes a rapid transition to turbulence following reattachment, as seen in both the shear stress distribution curve and in the shapes of profiles E and F.

Interactions investigated at Mach 3.0 and a Reynolds number of 6.0×10^6/m display similar characteristics under corresponding near-zero pressure gradient, incipient, small separation, and large separation conditions. These results are presented in Fig. 7. Due to the change in geometry, the shock impingement points are further downstream than observed for the Mach 2.0 data, although the interactions again are with laminar boundary layers for these cases.

Noticeable differences from that of the Mach 2.0 results are that the interaction-induced disturbances occur further upstream of the indicated shock impingement locations and that the lengths of the disturbance regions are greater.

The Mach 4.0 results likewise are generally similar to those obtained at Mach 2.0, but with the interaction occurring further upstream of shock impingement and with longer lengths of disturbance than realized at Mach 3.0.

The set of Reynolds number 9.5×10^6/m results at Mach 4.0 are found in Fig. 8, with the near-zero pressure gradient condition shown in Fig. 8a. Profiles A–C indicate an attached laminar boundary-layer condition, with the static pressure rise caused by leading-edge effects appearing misleadingly large here due to the scaling chosen. Incipient separation is shown in Fig. 8b, while laminar boundary layer separations produced by stronger interaction conditions are presented in Figs. 8c and 8d.

Additional results for the various Mach numbers can be found in Ref. 13.

Comparison of Results with Previous Work

As mentioned earlier, the study reported in Refs. 6 and 15 represents the most complete previous work on the subject of two-dimensional laminar shock/boundary-layer interactions. Direct comparison is not possible due to disparity in the Reynolds number ranges used in the present and previous work. One attempt to examine the two data sets for qualitative similarity of interaction phenomena, by selecting those cases for comparison having approximately the same separation lengths and reattachment behavior, is presented in Fig. 9. Here, the velocity profiles of the current report have been replotted and shear stress data scaled by a ratio of local Reynolds numbers in order to compensate for differences in conditions. Close agreement is noted for this incipient separation as well as for other separated interaction cases.

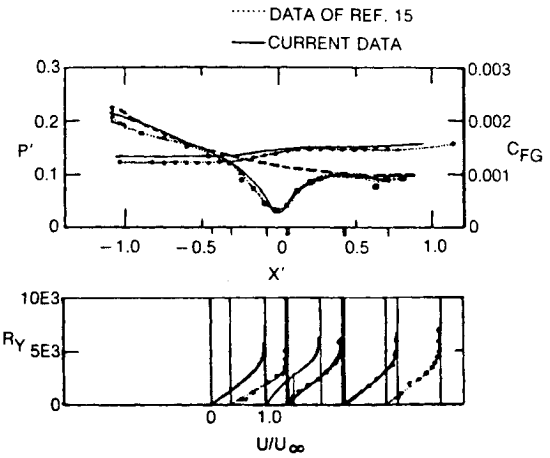

Fig. 9 Comparison of incipient separation distributions: current data and data of Greber.[15]

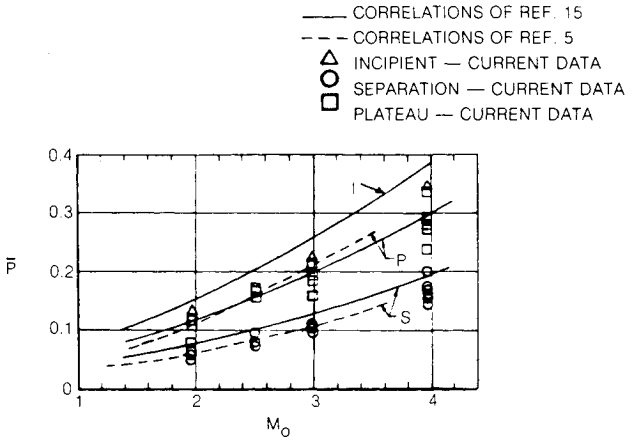

Fig. 10 Mach number effect on laminar separation characteristics.

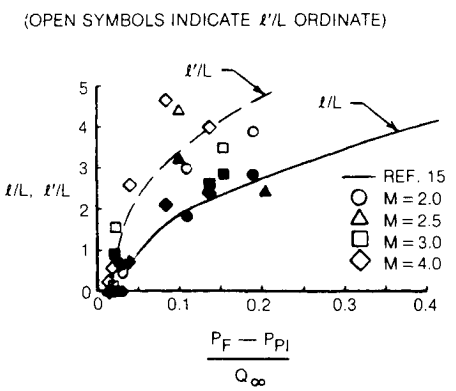

Fig. 11 Length of separated region in laminar boundary layer.

Correlations

Previous authors[5,15] developed correlations to describe incipient, plateau, and separation pressure using characteristics of the laminar boundary-layer interaction, with Ref. 5 deducing these by means of an extensive experimental program and Ref. 15 providing them through theoretical formulations based on a lifted layer analysis and by a momentum integral approach. Comparison of their correlations with the current experimental data is shown in Fig. 10. Correlation of separation length is examined in Fig. 11 by means of one of the variable sets (ℓ/L) recommended by Ref. 15. The correlation curve of Ref. 15 is plotted along with the current data and good agreement observed, especially considering the wide range of Mach and Reynolds numbers encompassed by the data, while the correlation itself was based solely on Mach 2.0 data at lower Reynolds number conditions. The data are also plotted and a correlation curve drawn in this figure based on the variable ℓ'/L, where ℓ' is the length of the separation determined from the shear stress curve fit, as this provides a more definite physical length. A complete discussion of the results of the experimental program is found in Ref. 13, along with a detailed examination of the accuracy of results.

Summary

Detailed information on the variation in flow properties through the regions of two-dimensional interactions between an oblique shock wave and primarily laminar flat-plate boundary layers has been obtained at a number of conditions within an overall freestream unit Reynolds number range of 4.72×10^6–2.95×10^7/m and for a Mach number range of 2.0–4.0. The current work provides a useful extension of earlier Mach 2.0 data to higher Reynolds numbers, as well as a detailed and documented body of information over a range of Mach numbers. The information is available in a form convenient for use by future investigators.

Acknowledgments

This work is part of a NASA Lewis Research Center program of "benchmark" experiments and was supported in part by NASA Grants NAG 3-61 and NAG3-102. Support for journal publication was provided by United Technologies Research Center.

References

[1]Ferri, A., "Experimental Results with Airfoils Tested in the High-Speed Tunnel at Guidonia," NASA TM 946, July 1940 (English translation from *Atti di Guidonia*, No. 17, Sept. 1939).

[2]Liepmann, H.W., "The Interaction Between Boundary Layer and Shock Waves in Transonic Flow," *Journal of the Aeronautical Sciences*, Vol. 13, Dec. 1946, pp. 623–638.

[3]Fage, A. and Sargent, R.F., "Shock-Wave and Boundary-Layer Phenomena Near a Flat Surface," *Proceedings of the Royal Society of London*, Ser. A, Vol. 190, June 1947, pp. 1–20.

[4]Barry, F.W., Shapiro, A.H., and Neumann, E.P., "The Interaction of Shock Waves with Boundary Layers on a Flat Surface," *Journal of the Aeronautical Sciences*, Vol. 18, April 1951, pp. 229–238, 270.

[5]Chapman, D.R., Kuehn, D.M., and Larson, H.K., "Investigation of Separated Flows in Supersonic and Subsonic Streams with Emphasis on the Effect of Transition," NACA TN-3869, March 1957.

[6]Hakkinen, R.J., Greber, I., Trilling, L., and Aberbanel, S.S., "The Interaction of an Oblique Shock Wave with a Laminar Boundary Layer," NASA Memo 2-18-58W, March 1959.

[7]Watson, E.C., Murphy, J.D., and Rose, W.C., "Investigation of Laminar and Turbulent Boundary Layers Interacting with Externally Generated Shock Waves," NASA TN D-5512, Nov. 1969.

[8]Reda, D.C. and Murphy, J.D., "Shock Wave/Turbulent Boundary Layer Interactions in Rectangular Channels," *AIAA Journal*, Vol. 11, Feb. 1973, pp. 139–140.

[9]Law, C.H., "Supersonic Shock Wave Turbulent Boundary-Layer Interactions," *AIAA Journal*, Vol. 14, June 1976, pp. 730–734.

[10]Shang, J.S., Hankey, W.L., and Law, C.H., "Numerical Simulation of Shock Wave-Turbulent Boundary-Layer Interactions," *AIAA Journal*, Vol. 14, Oct. 1976, pp. 1451–1457.

[11]Li, C.P., "A Numerical Study of Separated Flows Induced by Shock-Wave Boundary-Layer Interaction," AIAA Paper 77-168, Jan. 1977.

[12]Tassa, Y., Anderson, B.H., and Reshotko, E., "Interactive Calculation Procedure for Supersonic Flows," NASA TM X-73653, May 1977.

[13]Skebe, S.A., "Experimental Investigation of Two Dimensional Shock Boundary Layer Interactions," Ph.D. Dissertation, Case Western Reserve University, Cleveland, OH, Aug. 1983.

[14]Abarbanel, S.S., Hakkinen, R.J., and Trilling, L., "Use of a Stanton Tube for Skin-Friction Measurements," NASA Memo 2-17-59W, March 1959.

[15]Greber, I., "Interaction of Oblique Shock Waves with Laminar Boundary Layers," Ph.D. Dissertation, Fluid Dynamics Research Group, Massachusetts Institute of Technology, Cambridge, Tech. Rept. 59-2, April 1959.